Mine Water and the Environment (2021) 40:713–721
https://doi.org/10.1007/s10230-021-00760-8

TECHNICAL ARTICLE

Dynamic Response of a Non-Darcian Seepage System in the Broken Coal of a Karst Collapse Pillar

Tian-jun Zhang[1,2] · Ming-kun Pang[1,2] · Xiang Ji[1,2] · Hong-yu Pan[1,2]

Received: 22 January 2020 / Accepted: 4 February 2021 / Published online: 3 June 2021

Abstract

Dynamic research methods were used to assess the stability of non-Darcian seepage and verify that parameter changes are an important cause of mine water inrush due to a karst collapse pillar (KCP). A KCP is an infiltration system that contains a large amount of partially cemented crushed coal and rocks, and can be very dangerous. We analysed the influence of parameter changes on the stability, the initial permeability, the equilibrium flow velocity, and the deviation factor β to study the non-Darcian seepage characteristics of this crushed coal media system. The permeability parameters of the internal structure of a KCP were used to characterize the evolution of a KCP water inrush accident. In the physical tests, the porosity of the framework was the factor that determined the seepage state of the porous medium and the initial permeability of the framework. For mines with a risk of KCP water inrush, the permeability parameters also have a safe range. Numerical calculations verified that the system's equilibrium state was stable, and that it has two equilibrium flow rates v_{s2} (3.5×10^{-4} m/s) and v_{s3} (5.5×10^{-4} m/s); this interval will not cause a change in flow regime. Thus, the limiting value of the non-Darcian deviation factor β was defined given the experiment's initial conditions: when it is less than -1.5×10^{11} kg/m^4, the system is not in equilibrium, and the seepage system will lose stability.

Keywords Mine water inrush · Dynamic response · Water seepage · Permeability · Seepage loss

Introduction

A karst collapse pillar (KCP) is a special geological structure formed by sedimentation, dissolution, compaction and natural cementation of broken coal and rock due to long-term geological movement and groundwater (He et al. 2009; Ma et al. 2015). The internal filling of a KCP is easily affected by groundwater and can migrate, making these porous media structures extremely unstable. Water inrush can be caused by the destruction of the karst structure, forming a channel for groundwater inflow. If high-pressure water in an aquifer floods into the KCP, it can produce a water inrush disaster (Lu et al. 2015; Ma et al. 2017). As the speed of the water increases, the Forchheimer flow in the KCP is first dominated by viscous drag, which gradually transitions to combined viscous and inertial drag, and is ultimately dominated by inertial drag (Qi et al. 2017). From the perspective of seepage in porous media, it is believed that high-pressure groundwater can cause the water to flow through a KCP fast enough to create a non-linear, high-speed Forchheimer seepage field (Xue et al. 2018).

Scholars have carried out a lot of research on the management and model analysis of KCP water inrush accidents. Among them, Miao et al. (2007) proposed some water barrier models: lithologic water-resisting with a weak rock layer, structure water-resisting with a hard rock layer, and water-resisting with the fracture passage closing. Zhou et al. (2018) used a hierarchical analysis structure model of a deep well floor water inrush to calculate the weight of each influencing factor, and sorted these factors to determine the main factor of influence. These methods have certain feasibility, and to a certain extent can temporarily solve the problem of mine water inrush. However, the effects of geology and hydrology have caused the mechanical properties and permeability properties of KCPs to be quite different from those of general rock masses. Natural groundwater and the internal structure of a KCP are a coupled process of interaction and

✉ Ming-kun Pang
1063862886@qq.com

[1] College of Safety Science and Engineering, Xi'an University of Science and Technology, Xi'an 710054, China

[2] Key Laboratory of Western Mine Exploitation and Hazard Prevention of the Ministry of Education, Xi'an, China

mutual influence. Thus, it is necessary to study the seepage characteristic parameters of crushed coal media from the overall stability of the seepage system to better prevent and manage KCP water inrush accidents in mines, and analyse the causes of KCP water inrush accidents and the mechanisms of water inrush.

Considering that the seepage system composed of this crushed coal medium belongs to a complex nonlinear system, we analysed the core parameters, such as the porosity and permeability of the crushed coal medium system, by combining physical test and numerical calculation methods. Parameter ranges and critical parameters were obtained for maintaining steady-state permeability of the seepage system, providing the core judgment basis and reference values for predicting water inrush accidents. Furthermore, by measuring on-site parameters, such as water seepage volume, the number of infiltration channels, surrounding stress values and other parameters at mines with a risk of KCP water inrush, these accidents can be scientifically evaluated. Supplemental Figure S-1 shows the specific geological structure of the mine and the sampling location of the sample.

Collection of Basic Parameter Data

Test Equipment

We also independently designed and used a tri-axial seepage test system to accurately measure the initial permeability, k, and the deviation factor, β, to be used in the numerical calculation. Several initial seepage process parameters can be measured with the system including: flow Q, mass m, flow velocity v, pressure p, and time t. After conversion, many parameters required for the numerical calculation were obtained. A schematic diagram of the permeability meter is shown in supplemental Fig. S-2.

The KCP is a special geological phenomenon. It is formed by the deposition, compaction, and recementation of broken coal. Most of its structure is made of coarse particles. At higher hydraulic gradients and flow velocities, it often shows a non-Darcian seepage state, and so better understanding of the non-Darcian flow factor is important (Phanikumar et al. 2002; Zhang et al. 2018a). A large number of laboratory experiments have been carried out using a natural core as the flow skeleton and air or water as the flow medium to determine the size of the β coefficient, generally based on the Forchheimer empirical formula $J = av + bv^2$ (Cherubini et al. 2012; Ouyang et al. 2016); to measure non-Darcian flow β factors, many scholars (Evans 1994; Geertsma 1974; Li 2001; Macdonald 1979; Pascal 1980) established relevant empirical formulas through experimentation (Table 1).

Testing Process

In this test, the diameter of the produced sample was φ50 mm, the height was 50 mm, and coal particles were the sample material. Four sizes of coal particles were mixed with 50 g of cement, and shaped using a mold to create nine samples (M-1 to M-9), which was then representatively tested. The axial pressure was set at 0.1, 5, 10, 15, 20, 25, 30 KN, the chosen lateral pressure was 3 MPa, and the seepage pressure was 0.5, 1.0, 1.5, 2.0, 2.5, or 3.0 MPa. The speed of the permeate was directly tested using a tri-axial permeameter. By calculating the Reynolds number, the flow state during infiltration was preliminarily judged, and the permeability k_D in the Darcy state was calculated. The Forchheimer formula was used to calculate the k and β values in the non-Darcy state. The results of the seepage parameter measurements are shown in Table 2.

By analysing the phenomenon, we found that high porosity was associated with many channels inside the sample and a high flow velocity. When the porosity was small, most of the internal pore channels of the sample were sealed and the flow velocity was small. However, determination of the β-factor is currently limited to indoor physical tests, which cannot characterize the global response of the seepage system.

Calculation Method

The boundary conditions are more complicated for the water inrush problem caused by the special geological structure of a KCP, as the material is a discontinuous medium, which

Table 1 Different scholars' research results on β

Scholar's name	Test object (sample material)	Fitting formula
Geertsma J	Sandstone, limestone, dolomite	$\beta = 1.59 \times 10^3 \Big/ \sqrt{k}\phi^{5.5}$
Evans RD	Multiple porous media and gases	$\beta = 5.5 \times 10^9 / k^{1.25}\phi^{0.75}$
Li D	Nitrogen and tight sandstone	$\beta = 1.15 \times 10^9 / k\phi$
Macdonald IF	Multiple gases (CO_2, CH_4, H_2)	$\beta = 4.92 \times 10^6 \Big/ \sqrt{k}\phi^{1.5}$
Pascal H	Fractured rock mass (engineering test)	$\beta = 4.8 \times 10^{10} / k^{1.176}$

Table 2 Seepage parameter measurement result

Group	Parameter	Axial pressure *F*/KN						
		0.1	5	10	15	20	25	30
MK-1	φ/%	0.292	0.281	0.270	0.261	0.258	0.251	0.246
	k_D /μm^2	1.39	1.02	0.94	0.84	0.66	0.65	0.62
	k /μm^2	4.19	1.27	1.42	0.72	0.49	—	—
	β/m^{-1}	2.29e10	2.33e10	2.78e10	4.14e10	4.69e10	—	—
MK-2	φ/%	0.540	0.410	0.327	0.321	0.306	0.300	0.287
	k_D /μm^2	9.39	6.44	5.48	1.10	0.28	0.21	0.18
	k /μm^2	2.38	1.43	3.02	0.31	—	—	—
	β /m^{-1}	5.13e11	3.09e11	3.20e11	4.86e11	—	—	—
MK-3	φ/%	0.127	0.121	0.119	0.112	0.108	0.100	0.095
	k_D /μm^2	1.96	1.68	1.34	0.13	0.10	0.08	0.04
	k /μm^2	9.80	1.90	2.04	0.79	—	—	—
	β /m^{-1}	3.80e11	2.17e11	4.62e11	2.23e10	—	—	—

makes it quite difficult to establish an accurate model of the problem (Packard et al. 1980; Zhang et al. 2018b). At the same time, the field engineering environment is relatively complex and there are few kinetic signals that can be tested. Therefore, it is necessary to describe the dynamic characteristics of the system using several time series (Takens 1981; Wang et al. 2017). The specific process follows.

Construction of the Non-Darcy Seepage Equation

The governing equation of non-Darcian flow in a broken coal rock mass includes three equations to calculate mass conservation, seepage motion, and state of equilibrium. Wang et al. (2017) gives the numerical calculation format of the one-dimensional non-Darcy flow equation, which the equilibrium state of the system $(\overline{p}_s \overline{v}_s)$ satisfies:

$$\begin{cases} \dfrac{\partial \overline{v}_s}{\partial \overline{x}} = 0 \\ a_1 \dfrac{\partial \overline{p}_s}{\partial \overline{x}} + a_2 \overline{v}_s + a_3 \overline{v}_s^2 + a_4 = 0 \end{cases} \tag{1}$$

among them: $a_0 = \frac{1}{p_0 \phi_0 c_t}, a_1 = \frac{p_0}{\rho_0 c_a}\left(\frac{\rho g k}{\mu}\right)^2, a_2 = \frac{\rho g H}{\rho_0 c_a}, a_3 = a_2,$ and $a_4 = \left(\frac{\rho g k}{\mu}\right)^2 \cdot \frac{gH}{c_a}$. $\overline{v}_s$ represents the equilibrium seepage velocity; $\overline{p}_s$ represent the equilibrium seepage pressure; $\overline{x}$ indicates equilibrium displacement; a_0, a_1, a_2, a_3, a_4 are the new parameter introduced by the equation to simplify the coefficients; ϕ_0 represents the initial porosity; c_t represents the comprehensive compression factor; ρ_0 represents the initial density; and c_a represents the acceleration coefficient.

Initial conditions: pore pressure, $p_0(x) = p_{01} + \frac{p_{02}-p_{01}}{H}x$, $v_0(x) = v_0$. H is sample height; p_{01} and p_{02} are the initial seepage pressures of the upper and lower ends respectively. Boundary conditions: $p|_{x=0} = p_1$, $p|_{x=H} = p_2$, and $p_2 p_1$, the direction of seepage flows from bottom to top. The seepage model of broken coal is shown in Fig. 1.

Numerical Calculation Method

To solve the seepage equation, the following format was constructed. The partial derivative of $\bar{t}$ uses the forward difference formula, and the partial derivative of $\bar{x}$ uses the central difference formula, where i represents time and j represents displacement, resulting in:

$$\begin{cases} \overline{p}_{i+1,j} = \overline{p}_{i,j} + \Delta\bar{t} \cdot (-a_0)\dfrac{\overline{v}_{i,j+1} - \overline{v}_{i,j-1}}{2\Delta\bar{x}} \\ \overline{v}_{i+1,j} = \overline{v}_{i,j} + \Delta\bar{t} \cdot [-a_1 \dfrac{\overline{p}_{i,j+1} - \overline{p}_{i,j-1}}{2\Delta\bar{x}} - a_2\overline{v}_{i,j} - a_3\overline{v}_{i,j}^2 - a_4] \end{cases} \tag{2}$$

Iteration method: the successive over-relaxation method (SOR), among them $(0 < \omega < 1)$, where $\omega = 0.6$, is a correction of the Gauss–Seidel (G-S) method. First, setting the component $x_j^{(k+1)}(j = 1, 2, ..., i-1)$ of the known quantity $x^{(k)}$, then, use the G-S method to define the auxiliary quantity $\overline{x}_i^{(k+1)}$, the form is as follows:

$$\overline{x}_i^{(k+1)} = (b_i - \sum_{j=1}^{i-1} a_{ij}x_j^{(k+1)} - \sum_{j=1+1}^{n} a_{ij}x_j^{(k)}) \Big/ a_{ii} \tag{3}$$

Finally, the weighted average of $x_i^{(k)}$ and $\overline{x}_i^{(k+1)}$ is defined as $x_i^{(k+1)}$. From this process, an iterative formula for pore pressure $p_{i,j}$ and percolation velocity $v_{i,j}$ can be constructed in the form:

$$\begin{cases} p_{i,j+1} = p_{i,j} + \omega(\overline{p}_{i,j+1} - p_{i,j}) \\ v_{i,j+1} = v_{i,j} + \omega(\overline{v}_{i,j+1} - v_{i,j}) \end{cases} \tag{4}$$

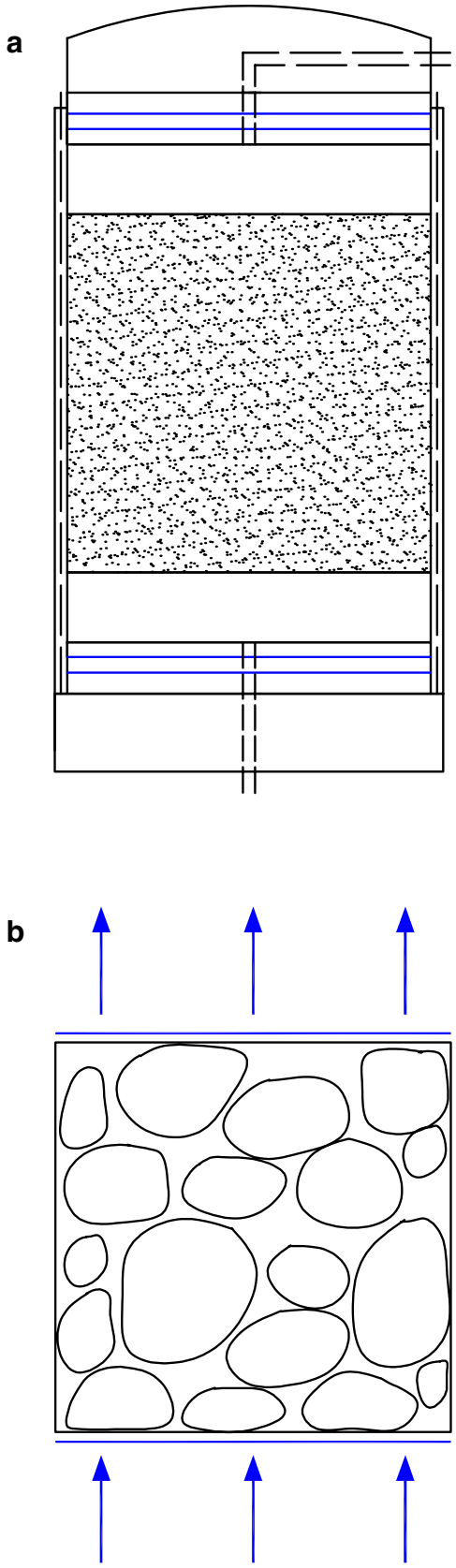

Fig. 1 Seepage model of broken coal: **a** sample seepage test process; **b** boundary conditions of seepage

The parameters in the SOR calculation process are the measured parameters, which are selected from the parameters of the coal and rock samples in the physical test. The details are shown in Table 3. The code was written in the FORTRAN language using the iterative format constructed above, and the points were iteratively calculated by the compiler, allowing the time series of the pore pressure and the percolation velocity of each node to be obtained.

Results and Discussion

Water inrush accidents are also a phenomenon of instability. The essence of stability lies in the permeability parameters (permeability k, non-Darcy β, pore pressure P, flow velocity v, and seepage pressure p). So, we analysed the stability of the equilibrium solution of the equation, the time series of pore pressure, and the velocity of the seepage system. Wang et al. (2017) gave three solutions of the system, for the three intervals: $\beta > 0$, $\beta_s < \beta < 0$, and $\beta < \beta_s$, which we combined with the test results.

Parameter Analysis of the Seepage System in Steady State.

(1) First, we studied the stability of the seepage system in the initial state, at this stage: $\beta > 0$. At this time, the non-Darcian flow deviates from the factor $\beta = \beta_0$, and bring in the initial parameters measured in the experiment to get the value 1.5×10^{11} in equilibrium. The seepage velocity, $v = v_0$, and for the initial parameters measured in the experiment yields an equilibrium seepage velocity of 6.1×10^{-4}. Next, the initial water pressure is offset by a small amount to give an initial boundary initial pore pressure of 0.2 MPa and a lower boundary initial water pressure, deviating from the equilibrium state of 0.002 MPa. The pore pressure history curve and the seepage velocity history curve obtained by iterative calculation follows the steady attractor law (Fig. 2).

Figure 2a shows the time series of the pressure p when the non-Darcian flow in the equilibrium state deviates from the factors β_0 and v_0. Since the initial pore pressure was disturbed by 0.002 MPa, the pre-seepage pressure p exhibits a certain amplitude fluctuation, the medium-term fluctuation amplitude gradually decreases, and later stabilizes. Figure 2b shows the time series of the seepage velocity v. From the curve change trend, it can be obtained that the seepage velocity generally shows a downward trend until it finally stabilizes. Observe that even if it is subject to a small disturbance, the system solution for the equilibrium state can still be stabilized.

(2) To further study the stability of the equilibrium state, the non-Darcian flow deviation factor $\beta = 1.5 \times 10^{11}$ was still used, as was the pore pressure equilibrium value, $p_1 = 0.6$ MPa, $p_2 = 0.2$ MPa. Next, given the initial percolation velocity v_0, there is a small offset near the steady-state

Table 3 Parameter selection

Parameter	Value	Parameter	Value
Initial porosity/ φ_0	0.33	Accelerating factor/ c_a	9.5×10^{9}
Initial pressure/ p_0	0.4 MPa	Pore compressibility/ c_φ	2.0×10^{-9} Pa^{-1}
Boundary pressure/ p_1, p_2	0.6, 0.2 MPa	Liquid compressibility/ c_f	4.8×10^{-10} Pa^{-1}
Poisson ratio/ μ	1.0×10^{-3} (Pa·s)	Density/ ρ_0	1000 (kg/m^3)
Permeability/ k	0.5×10^{-13} m^2	Height element/$\Delta\bar{x}$	0.1
Non-Darcy factor/ β_0	1.5×10^{11} ($kg\cdot m^{-4}$)	Time element/$\Delta\bar{t}$	1.1×10^{-3}
Height/ H	5.0 m	Elaxation factor/ ω	0.5

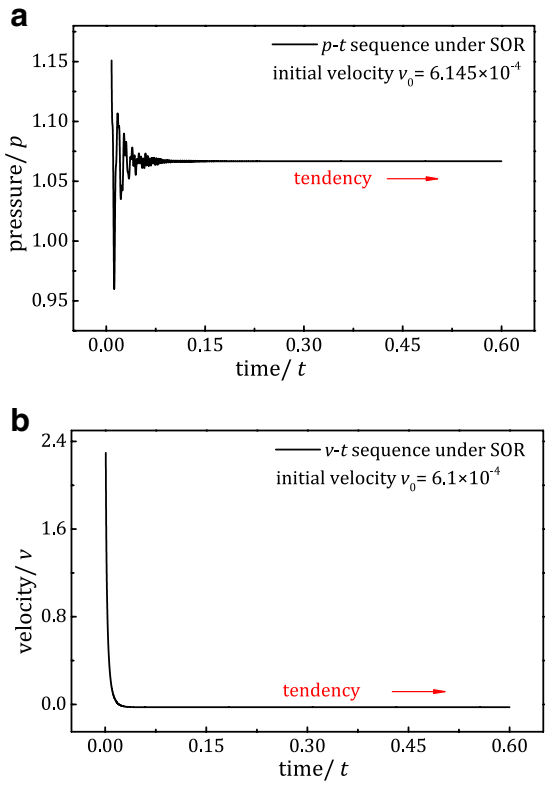

Fig. 2 Constant attractor: **a** p–t curve (non-dimensional); **b** v-t curve (non-dimensional)

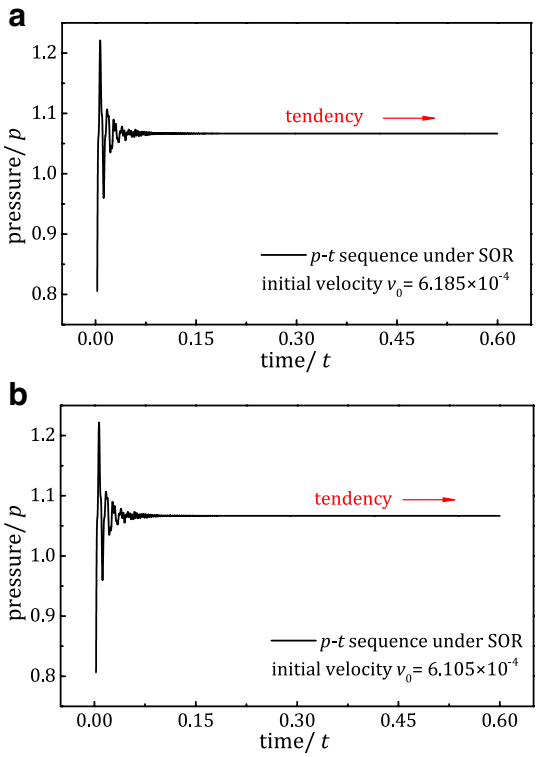

Fig. 3 Equilibrium attractor: **a** upward velocity deviation (non-dimensional); **b** downward velocity deviation (non-dimensional)

flow rate of 6.1×10^{-4}, the upper offset value is 6.2×10^{-4}, and the lower offset value is 6.1×10^{-4}. The pore pressure history curve obtained by iterative calculation is the law of equilibrium attractor change (Fig. 3).

Figure 3 shows the stability of the system near a given initial percolation velocity, $v_0=6.1\times10^{-4}$. Figure 3a shows the offset *p–t* characteristic curve on the percolation velocity, and Fig. 3b shows the percolation velocity offset *p–t* characteristic curve. It can be seen from the curve that the offset and lower offset of the percolation velocity in the equilibrium state can be stabilized to a certain value. Relatively speaking, for the same amplitude disturbance, the time required for the up-offset disturbance to stabilize is short, while the time for the down-offset disturbance to stabilize is long. However, overall the system can be stabilized.

(3) To further study the stability of this system, we first chose an initial value ($v=6.145\times10^{-4}$), and then chose a β value in the range of the equilibrium state ($\beta>0$), and analysed the change of β value to the system stability influence of state, again assuming the equilibrium value pore pressure. Next, the non-Darcy flow deviation factor β value was continuously increased, and set at 1.5×10^{11} and 1.45×10^{12}. The pattern of seepage velocity and pore pressure obtained by iterative calculation is that of the phase trajectory change. Figure 4 shows the phase trajectories corresponding to different β values when the system is in equilibrium.

Analysis of the curve shows that at the initial stage, regardless of any rate of attenuation, the final phase

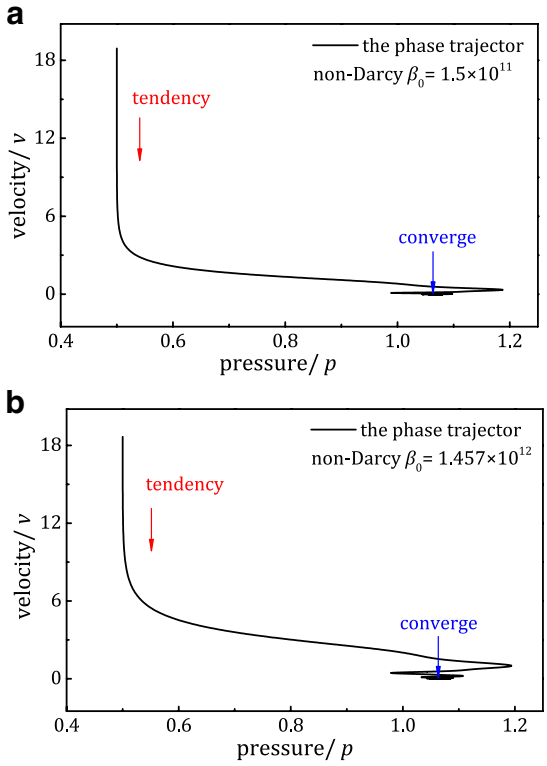

Fig. 4 Phase trajectories at different β values: **a** β0 = 1.5 × 1011 (non-dimensional); **b** β0 = 1.5 × 1012 (non-dimensional)

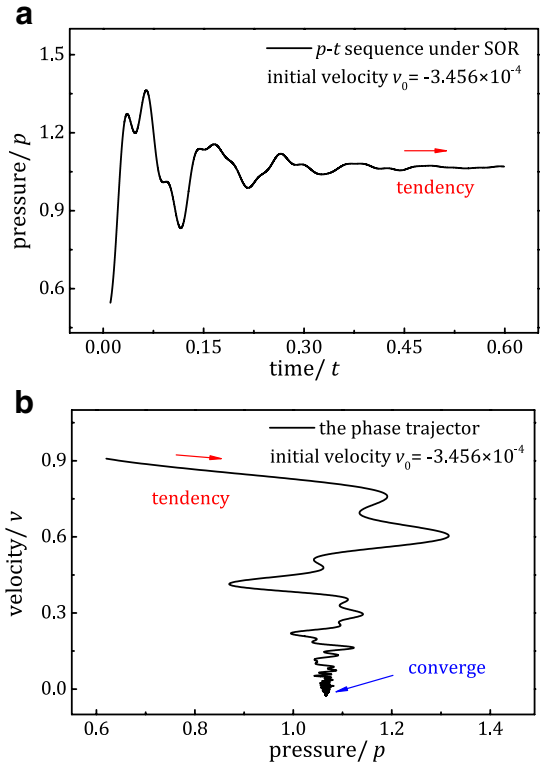

Fig. 5 Stability near speed v_{s1}: **a** p–t curve (non-dimensional); **b** the phase trajectory (non-dimensional)

trajectory can converge to an area, that is, the focal point, and the seepage system is safe. If the value of β continues (Fig. 4a), the time for the curve to reach convergence is faster than in Fig. 4b, but the location (coordinates) of the convergence point is basically the same. Thus, by analysing the parameters, we found that the seepage system at this stage is stable. Therefore, no matter how the parameters change (including the permeability of the KCP structure, the permeability rate, and the porosity of the structure), the risk of a KCP water inrush will not quickly change, and the system at this stage is safe.

Parameter Analysis of a Seepage System in a Transitional State.

At this stage: $\beta_s < \beta < 0$. Considering that the non-Darcian flow deviation factor $\beta < 0$, the system has two equilibrium states, which can be calculated according to the parameters k, c_a, H, p_1, p_2, μ, ρ_0, etc. set earlier. For v_{s1} (-3.5×10^{-4} m/s) and v_{s2} (-5.5×10^{-4} m/s), the limit parameter β_s (-1.5×10^{11} kg/m^4) can also be calculated using the above parameters. Therefore, given a small disturbance of speed, set at $v_0 = -3.5\times10^{-4}$, and the stability near the equilibrium state v_{s1} is as shown in Fig. 5.

With a small disturbance near the equilibrium state velocity, v_{s2} (-5.5×10^{-4} m/s), and $v_0 = -5.5\times10^{-4}$, we obtain the corresponding pore pressure time series by iteration. The pattern of the phase trajectory reflects its stability, and the corresponding phase line is as shown in Fig. 6.

Two equilibrium velocities v_{s1} and v_{s2} are obtained by calculation. Figure 6 studies the stability near the speed v_{s2}. The results show that at this stage ($\beta_s < \beta < 0$), the response curves showed large fluctuations. Analysing Fig. 5a, the curve takes a long time to converge; for Fig. 6a, the curve fluctuates greatly, and there is even a trend of non-convergence; this gap in the convergence trend leads directly to Fig. 5b. The phase trajectory pattern presented in Fig. 6b does not converge, which shows that the stability of the seepage system at this stage has a lot to do with the parameters, which each has a certain limit; if the limit is exceeded, the system will be unstable. We have no way to observe the evolution of KCP for several years, but we can characterize the evolution of a KCP water inrush accident from the perspective of the stability of the seepage equation. This shows that at a mine with a risk of a KCP water inrush accident, a continuous increase in water seepage volume and a deformation of the seepage structure, a new channel inside can be generated, which is dangerous for the mine.

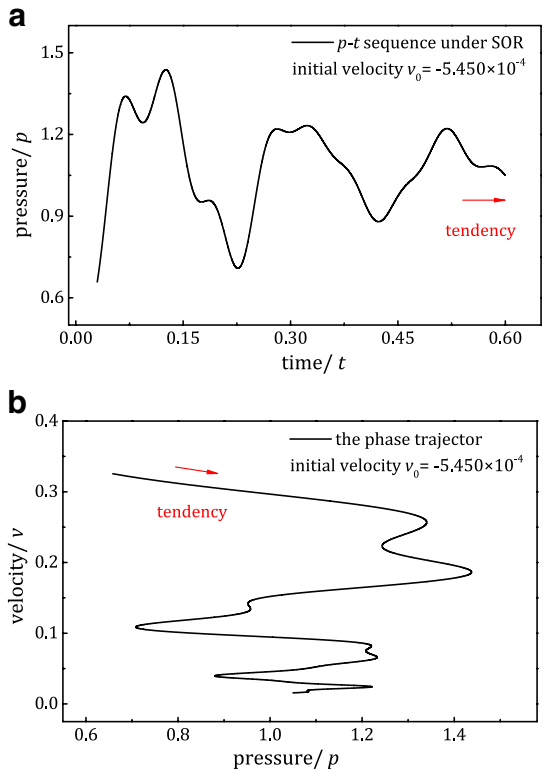

Fig. 6 Stability near speed v_{s2}: **a** p–t curve (non-dimensional); **b** the phase trajectory (non-dimensional)

Parameter Analysis of the Seepage System in an Unstable State

At this stage: $\beta < \beta_s$. Considering the non-Darcian flow state, the inertial force received by the fluid will directly affect the system seepage parameters. If the non-Darcian flow deviation factor β is less than the limit parameter β_s (-1.5×10^{11} kg/m^4), there is no equilibrium. Here, the β value is -1.5×10^{12}, and the time series of the seepage velocity and the time series of pore pressure at this stage are studied, as shown in Fig. 7a and b. Therefore, we studied the dynamic characteristics of the system at the initial velocity $v_0=2.6\times10^{-6}$ and at the small velocity $v_0=2.6\times10^{-12}$. The dynamic characteristics of the instability phase are as shown in Fig. 7.

Figure 7a shows that the pore pressure at this stage will tend to infinity, while Fig. 7b shows that the seepage velocity at this stage does the same. The fundamental reason for this is that the system does not have a steady-state seepage stage due to the damage to the simulated KCP. The system still shows a divergent trend when the value of β is increased by an order of magnitude, and on this basis, the disturbance value continues to decrease, as shown in Fig. 7c and d. The phase trajectory patterns are basically the same, and the final ones flow to infinity, indicating that the system is unstable at this stage. No matter how the parameters are selected, the system will become unstable, and any change in the KCP structure will induce a water inrush accident. This feature also reminds us that if we observe unstable water seepage and an extremely unstable structure while field testing mines with a water inrush risk, and the calculated parameters of each parameter exceed the critical value, we can consider the KCP structure at the location to be very risky. Mining must stop until preventive action (e.g. grouting) is completed. When the structure is stable, the seepage volume will be small, and production can begin again. Still, it should be recognized that the KCP has evolved to a very dangerous state and that a small stress disturbance could cause a large amount of water to appear in the mine.

Conclusions

The evolution of a KCP water inrush accident is affected by various conditions. In this study, the characteristics of non-Darcian flow were considered, and the corresponding coefficients (permeability, initial porosity, grain size distribution, etc.) were addressed through physical tests and numerical calculations. Key factors affecting the stability of the system were establish and verified. The essential reasons leading to system instability were analysed from the perspective of parameter mutation, which will provide a theoretical basis for the prediction and management of later water inrush accidents. The conclusions are as follows:

(1) Using physical simulations of a KCP, physical test method, the fundamental factor for determining the seepage state is the porosity of the skeleton, which reflects the number and size of the pore channels inside the sample. When the channel increases, the flow rate decreases, and Darcy's law is established. When the pore channel is closed, the flow rate is small, so the physical test method cannot accurately determine the β factor, and the global characteristics of the seepage system cannot be characterized.

(2) Therefore, the numerical calculation method was used to study this special geological structure, revealing the evolution process of a KCP water inrush accident from the changes in the permeability characteristics of the structure. Using the numerical calculation method, the stability of the solution under the system equilibrium state was verified, and the safety parameter range of a broken coal media system was characterized. When $\beta>0$, the system has an equilibrium flow velocity v_0 (6.1×10^{-4} m/s); when $\beta_s<\beta<0$, the system has two equilibrium flow rates v_{s1} (3.5×10^{-4} m/s) and v_{s2} (5.5×10^{-4} m/s), and even with small disturbances, these solutions are stable.

(3) Combined with the basic parameters of the physical test, the limit value of the non-Darcian deviation factor β was calculated. In the non-Darcian flow state, the inertial

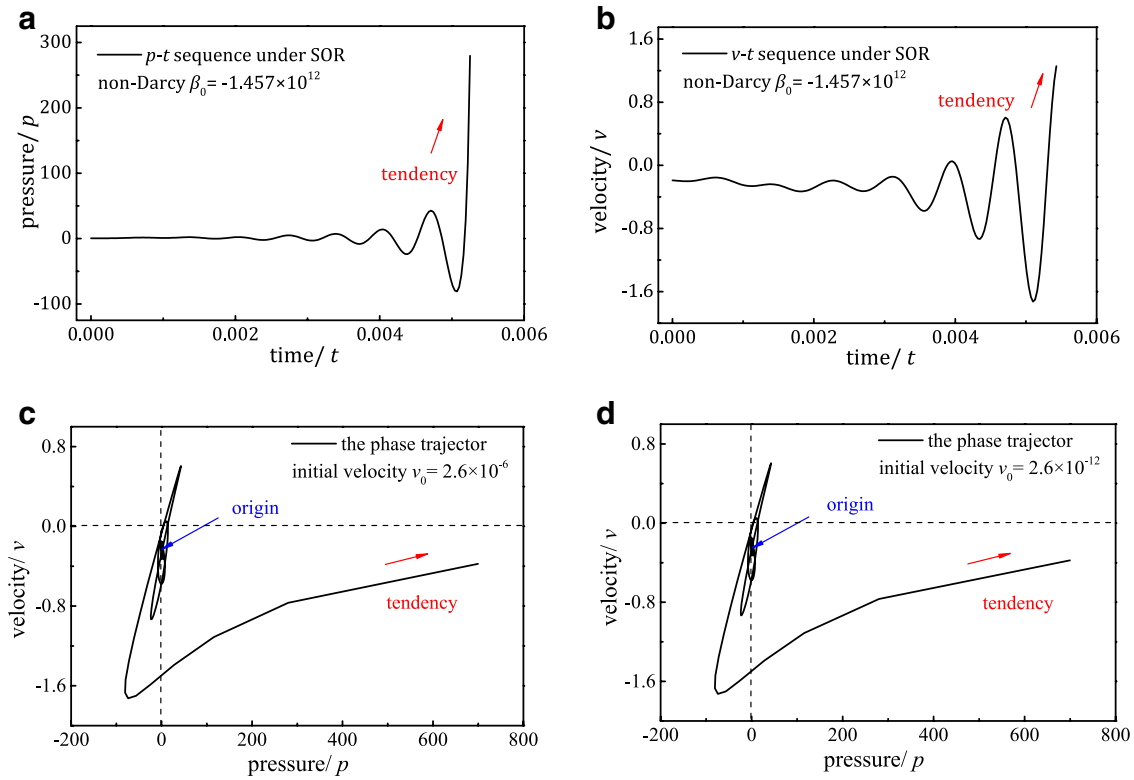

Fig. 7 Dynamic characteristics of the system instability stage: **a** *p–t* curve (non-dimensional); **b** *v-t* curve (non-dimensional); **c** v0 = 2.6×10^{-6} (non-dimensional); **d** v0 = 2.6×10^{-12} (non-dimensional)

force of the fluid directly affects the system seepage parameters. If β is less than the limit parameter β_s (-1.5×10^{11} kg/m^4), the system will be unstable. In this state, any sudden change of parameters will directly change the seepage flow pattern. The original seepage path will be further destroyed, new seepage channels will be produced, and the mine could be subject to water inrush accidents at any time.

Supplementary Information The online version contains supplementary material available at https://doi.org/10.1007/s10230-021-00760-8.

Acknowledgements This work was supported by the National Natural Science Foundations of China, Study on the Mechanism of Water-Gas Coupling Fracture Expansion and Ultrasonic Characteristics of Coal Rock Mass in Drilling Holes (Grant 51774234) and the Study on Mechanism and Parameter Optimization of Carbon Dioxide Deep Hole Pre-cracking Blasting (Grant 51874234).

References

Cherubini C, Giasi CI, Pastore N (2012) Bench scale laboratory tests to analyze non-linear flow in fractured media. Hydrol Earth Syst Sci 16(8):2511–2522

Evans RD, Civan F (1994) Characterization of non-Darcy multiphase flow in petroleum bearing formation. J Petrol Geol Eng 6(1):1538–1549

Geertsma J (1974) Estimating the coefficient of inertial resistance in fluid flow through porous media. Soc Petrol Eng J 14(5):445–450

Keqiang H, Guangming Y, Yaoru L (2009) Palaeo-karst collapse pillars in northern China and their damage to the geological environments. Environ Geol 58(5):1029–1040

Li D, Svec RK, Engler TW, Grigg RB (2001) Modeling and simulation of the wafer non-Darcy flow experiments. Proc SPE Western Reg Meet. https://doi.org/10.2118/68822-MS

Lu Y, Wang L (2015) Numerical simulation of mining-induced fracture evolution and water flow in coal seam floor above a confined aquifer. Comput Geotech 67:157–171

Ma D, Bai H (2015) Groundwater inflow prediction model of karst collapse pillar: a case study for mining-induced groundwater inrush risk. Nat Hazards 76(2):1319–1334

Ma D, Rezania M, Yu H, Bai H (2017) Variations of hydraulic properties of granular sandstones during water inrush: Effect of small particle migration. Eng Geol 217:61–70

Macdonald IF, El-Sayed MS, Mow K, Dullien FAL (1979) Flow through porous media-the Ergun equation revisited. Ind Eng Chem Fund 18(3):199–208

Miao X, Chen R, Bai H (2007) Fundamental concepts and mechanical analysis of water-resisting key strata in water-preserved mining. J China Coal Soc 6:74–97

Ouyang Z, Liu D, Cai Y, Yao Y (2016) Investigating the fractal characteristics of pore-fractures in bituminous coals and anthracites through fluid flow behavior. Energy Fuel 30(12):10348–10357

Packard NH, Crutchfield JP, Shaw RS (1980) Geometry from a time series. Phys Rev Lett 45:712–734

Pascal H, Quillian RG (1980) Analysis of vertical fracture length and non-Darcy flow coefficient using variable rate tests. Proc SPE Ann Tech Conf Exhibit. https://doi.org/10.2118/9348-MS

Phanikumar MS, Mahajan RL (2002) Non-Darcy natural convection in high porosity metal foams. Int J Heat Mass Tran 45(18):3781–3793

Qi Y, Li M, Li K, Jim TC (2017) Spatiotemporal development of mine water inrush and its mechanism-a case study in Ganhe coal mine, Shanxi. China Arab J Geosci 10(19):433

Takens F (1981) Detecting strange attractors in turbulence. Springer-Verlag, Berlin

Wang L, Chen Z, Kong H (2017) An experimental investigation for seepage-induced instability of confined broken mudstones with consideration of mass loss. Geofluids 2017:1–12

Xue Y, Teng T, Zhu L, He M (2018) Evaluation of the non-Darcy effect of water inrush from karst collapse pillars by means of a nonlinear flow model. Water 10(9):1234

Zhang T, Bao R, Li S, Zhang C, Zhang L (2018a) Expansion properties and creep tests for a new type of solidified expansive sealing material for gas drainage boreholes in underground mines. Environ Earth Sci 77(12):468–481

Zhang T, Zhang L, Li S, Liu J, Pan H, Ji X (2018b) Wave velocity and power spectral density of hole-containing specimens with different moisture content under uniaxial compression. Energies 11(11):3166–3179

Zhou Z, Cai X, Ma D, Cao W, Chen L, Zhou J (2018) Effects of water content on fracture and mechanical behavior of sandstone with a low clay mineral content. Eng Fract Mech 193:47–65